ENVIRONMENTAL RESEARCH
LETTERS

LETTER • OPEN ACCESS

Regional sources control dust in the mountain critical zone of the Great Basin and Rocky Mountains, USA

To cite this article: Jeffrey S Munroe *et al* 2023 *Environ. Res. Lett.* **18** 104034

ENVIRONMENTAL RESEARCH
LETTERS

LETTER

Regional sources control dust in the mountain critical zone of the Great Basin and Rocky Mountains, USA

Jeffrey S Munroe[1,*], **Elsa J Soderstrom**[1], **Camryn L Kluetmeier**[1], **Michael J Tappa**[2], **Derek V Mallia**[3] and **Ann M Bauer**[2]

[1] Department of Earth & Climate Sciences, Middlebury College, Middlebury, VT 05753, United States of America
[2] Department of Geosciences, University of Wisconsin-Madison, Madison, WI 53706, United States of America
[3] Department of Atmospheric Sciences, University of Utah, Salt Lake City, UT 84112, United States of America
[*] Author to whom any correspondence should be addressed.

E-mail: jmunroe@middlebury.edu

Keywords: dust, critical zone, mountain environments, Southwestern US

Supplementary material for this article is available online

OPEN ACCESS

RECEIVED
14 August 2023

REVISED
14 September 2023

ACCEPTED FOR PUBLICATION
19 September 2023

PUBLISHED
28 September 2023

Abstract

Mountain environments are profoundly impacted by the deposition of mineral dust, yet the degree to which this material is far-traveled or intra-regional is typically unclear. This distinction is fundamental to model future changes in mountain geoecosystems resulting from climatic or anthropogenic forcing in dust source regions. We address this question with a network of 17 passive dust samplers installed in primarily mountain locations in Utah, Nevada, and Idaho between October, 2020 and October 2021. For each collector, the dust deposition rate was calculated, and the physical and chemical properties of the dust were constrained. Results were combined with backward trajectory modeling to identify the geologic characteristics of the area over which air passed most frequently in route to each collector (the 'hot spot'). Dust properties differ significantly between collectors, hot spots for many collectors are spatially discrete, and the dominant geologies in the hot spots corresponding to each collector vary considerably. These results support the hypothesis that the majority of the dust deposited in the areas we studied is sourced from arid lowlands in the surrounding region.

1. Introduction

The health and functioning of mountain ecosystems have broad societal relevance, given the importance of these environments as sources of fresh water and timber, wildlife habitat, recreational destinations, and as economic engines (Grêt-Regamey *et al* 2012, Egan and Price 2017, Grêt-Regamey and Weibel 2020). Research has demonstrated that the critical zone (CZ) in mountain environments is profoundly impacted by the deposition of allochthonous mineral dust, which alters the chemistry of surface water (Psenner 1999, Carling *et al* 2012, Brahney *et al* 2013, 2014), influences trajectories of soil formation (Dahms 1993, Lawrence *et al* 2011, 2013, Munroe *et al* 2015, 2020), provides nutrients necessary for plant growth and aquatic productivity (Brahney *et al* 2014, Aciego *et al* 2017, Arvin *et al* 2017), and alters the timing and rate of snowmelt (Painter *et al* 2007, 2010, Skiles *et al* 2018). These impacts are expected to become more acute in coming decades as more intense droughts, driven by climate change, increase the likelihood of wind-erosion and dust emission from arid landscapes (Cook *et al* 2020).

Mineral dust typically contains a range of particle sizes reflecting transport distance and the strength of the turbulence responsible for sustaining mineral grains in suspension (Adebiyi *et al* 2022, Vandenberghe 2013, Mahowald *et al* 2014, p 201). In many mountain settings, dust size distributions straddle the informal boundaries commonly used to distinguish fine ('small') far-traveled dust from coarse ('large') dust more likely to be regionally sourced (Stuut *et al* 2009). Far-traveled material would be expected to geochemically homogenous due to mixing during transport, whereas more regionally

derived dust should reflect the geology of specific source areas (Guieu *et al* 2002, Fitzgerald *et al* 2015). A central question in studies of mountain dust, therefore, is the relative importance of regionally sourced material with spatially varying properties, and far-traveled material that could be well-mixed and uniform over large regions.

Previous work has demonstrated situations in which either regional or far-traveled dust are dominant. For instance, in southwestern North America, dust arriving in the San Juan Mountains of Colorado typically originates from the Colorado Plateau, which is located directly upwind (Painter *et al* 2007, Neff *et al* 2008). In contrast, dust reaching the Colorado Front Range, on the eastern side of the Continental Divide, has be linked to agricultural and urban activity to the east (Heindel *et al* 2020). In New Mexico, dust from White Sands National Monument has been traced to the Sacramento Mountains ∼75 km away (Rea *et al* 2020). In northern Utah, the geochemistry and isotopic fingerprint of dust were shown to match dust-emitting landscapes in western Utah and parts of Nevada (Carling *et al* 2012, Goodman *et al* 2019, Munroe *et al* 2019). Yet at the other extreme, Saharan dust routinely crosses the Mediterranean and joins dust from China in reaching the Alps (Grousset *et al* 2003, Di Mauro *et al* 2019, Greilinger and Kasper-Giebl 2021), and non-trivial amounts of Asian dust arrive in the Sierra Nevada of California after trans-Pacific transport (Ault *et al* 2011, Creamean *et al* 2013, 2014, Aarons *et al* 2019). Collectively, these studies illuminate the ubiquity of dust transport to the mountain CZ over a broad range of spatial scales. However, because the physical and chemical variability of mountain dust over a wide region have not been systematically evaluated, uncertainty remains regarding the degree to which the properties of dust deposited in high-elevation settings varies between mountain ranges. This fundamental knowledge gap challenges attempts to model the effects of contemporary dust deposition in the mountain CZ, and to predict how these dust-influenced systems will evolve in the future.

Here we evaluate the degree to which flux and properties of mineral dust arriving in the mountain CZ of southwestern North America are controlled by the geology of the surrounding lowlands. Field measurements, remote sensing, and modeling efforts have established that dust deposition is an active process in this region (e.g. Nicoll *et al* 2019, Kok *et al* 2021), but it is unclear whether this dust is primarily delivered by global atmospheric circulation or intra-regional transport (figure 1(a)). Working with a network of samplers, we test the null hypothesis that dust properties are uniform across this region, as would be expected for far-travelled, globally-sourced, well-mixed material (figure 1(b)). Our alternate hypothesis is that dust deposited in the mountain ranges represented by our samplers is primarily derived from the surrounding area, and would therefore have spatially varying physical and chemical properties reflecting the geologies of unique sources (figure 1(c)).

2. Methods

2.1. Study design

We deployed an array of 17 passive dust samplers (supplemental figure 1) constructed following published designs (Munroe 2022a) primarily in mountain locations in the southwestern United States (figure 2). In northern Utah, samplers were deployed in the Uinta Mountains (samplers DUST-1 through DUST-8), the Wasatch Mountains (DUST-9), and at lower elevations in Salt Lake City (DUST-10) and in Provo (DUST-17). In southern Utah, samplers were installed in the Tushar Range (DUST-13) and in the La Sal Mountains (DUST-14). In eastern Nevada, samplers were located in the South Snake Range (DUST-12), the Ruby Mountains (DUST-11), and the Independence Range (DUST-15). A final sampler (DUST-16) was deployed in the Albion Range of southern Idaho (table 1).

Samplers DUST-1 through DUST-14 were in operation from fall 2020 through June 2021; all but DUST-14 were emptied in early July of 2021 to yield a winter dust sample (DUST-14 was inaccessible due to wildfire). Samplers DUST-15, DUST-16, and DUST-17 were added in the summer of 2021. All samplers were emptied in the fall of 2021 to yield 16 summer dust samples plus an annual sample from DUST-14. The deployment of the collectors for months at a time provides a perspective germane for functioning of the CZ, midway between event-scale sampling, such as dust on snow layers (Lawrence *et al* 2010), and the long-term averaging provided by soil and lake sediment studies (Neff *et al* 2008, Lawrence *et al* 2011, Routson *et al* 2019, Munroe *et al* 2021). The overall dataset contains 30 samples: 13 winter dust (October, 2020 through June, 2021), 16 summer dust (July through September, 2021), and 1 annual composite (table 1).

2.2. Analytical methods

All samples were evaluated in the laboratory following a consistent set of analyses intended to permit a rigorous comparison of the dust collected at the 17 locations. The depositional flux of mineral material was calculated from the dry mass after removal of organic material. Particle size distribution of the dust was determined with laser scattering, and dust color was quantified using standard CIELAB nomenclature. The mineralogy of the dust was investigated using x-ray diffraction (XRD), dust geochemistry was determined with inductively coupled plasma mass spectrometry (ICP-MS), and an isotope fingerprint

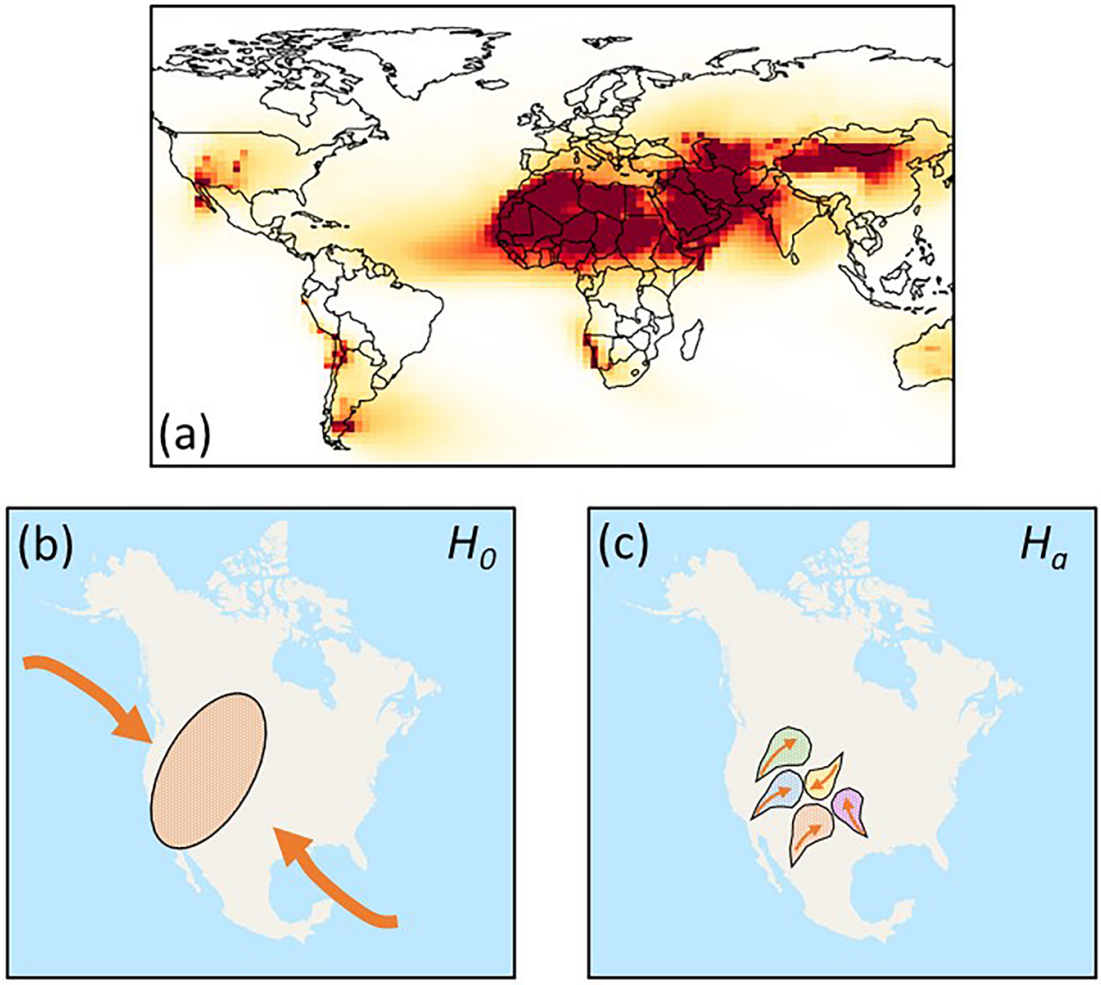

Figure 1. (a) Global map of modeled PM_{10} deposition (from Kok *et al* 2021). Dust transport operates at overlapping local to global scales, resulting in uncertainty about the relative balance of global and regional dust in a given area. (b) Schematic presenting the null hypothesis (H_0) that dust deposited in mountain regions of the southwestern United States is primarily globally sourced, well-mixed, and uniform. (c) Schematic presenting the alternate hypothesis (H_a) that dust reaching these mountains is dominantly derived from the surrounding lowlands, producing spatial variability in dust properties reflecting the geologies of unique source areas.

for each sample was defined using the radiogenic isotope metrics $^{87}Sr/^{86}Sr$ and ε_{Nd}. Full details of these methods are presented in the supplemental methods.

Given the number of samples, and the uneven size of the seasonal collections, non-parametric tests were used to determine the significance ($P < 0.05$) of differences between seasons. A Mann–Whitney U test was used for overall differences between winter and summer dust; a Wilcoxon signed-rank test was used for paired seasonal samples from DUST-1 through DUST-13.

HYSPLIT-STILT modeling produced a footprint map for each collector (Lin 2003, Loughner *et al* 2021), with concentrations in ppm/[μmol m^{-2} s^{-1}]. In a GIS, this output was contoured to delineate the 'hot spot' surrounding each collector, and this hot spot was used to clip a geologic map. The areas of different generalized bedrock types within the 'hot spot' for each collector were then summarized.

3. Results

We observe large spatial and temporal differences in depositional flux, and in physical and chemical properties, of the mineral material collected by our samplers (Munroe 2022b). Across the study area, dust is accumulating at rates of 5.3 to >250 mg m^{-2} d^{-1} (figures 3 and 4). The overall average flux is significantly greater ($P < 0.001$) during the summer (mean of 49.0 mg m^{-2} d^{-1}) compared with winter (17.5 mg m^{-2} d^{-1}). The highest summer flux was recorded by DUST-10 in Salt Lake City (255 mg m^{-2} d^{-1}), whereas the lowest fluxes were at DUST-9 and DUST-12 (<16 mg m^{-2} d^{-1}). In winter the greatest flux was also at DUST-10 (102 mg m^{-2} d^{-1}), with the second highest value at DUST-9 in the Wasatch Mountain immediately downwind (27 mg m^{-2} d^{-1}). As noted in previous work (Heindel *et al* 2020), dust flux tends to

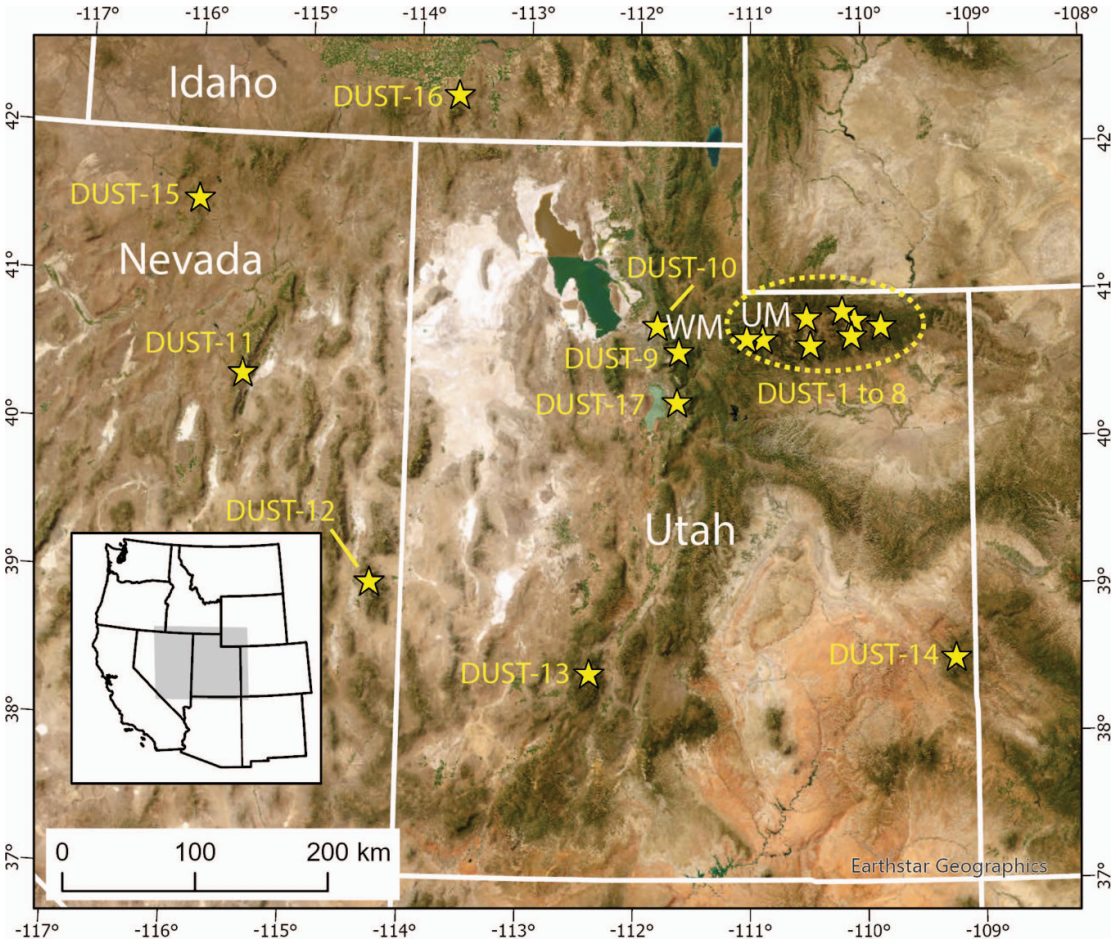

Figure 2. (A) Locations of the 17 passive dust collectors (yellow stars). The oval surrounds DUST-1 through DUST-8 in the Uinta Mountains (UM) of northeastern Utah. The north–south trending Wasatch Mountains are noted as 'WM'. Inset shows the location of the larger map (gray box) within the western US.

increase with elevation. However, some of this relationship is driven by the high fluxes at the lowest elevation near-urban sites in northern Utah. The overall geographic pattern is high values near Salt Lake City, intermediate values in northeastern Utah, and low values across southern Utah and eastern Nevada (figure 3).

The median grain size of all dust is 9.9 μm (6.6 φ), with 29% of the volume of each sample in the very fine silt (2–7 μm) size class (figure 4, supplemental figure 2). Abundances of total particulate <10 μm (PM_{10}) range from 28.7 to 69.8%, with $PM_{2.5}$ ranging from 9.2% to 21.9% (figure 4). In the seasonal paired samples from DUST-1 through DUST-13, values of medium and fine silt are significantly greater in winter ($P = 0.005$), whereas very fine silt is significantly more abundant in summer ($P = 0.043$). The coarsest median grain size in both seasons is at DUST-10 in Salt Lake City. In winter, the DUST-11 and DUST-12 sites in eastern Nevada are somewhat coarser than most Uinta sites and DUST-13. In summer, the eastern Nevada sites are notably coarser than all of the Uinta collectors.

In CIELAB nomenclature (L^*, a^*, b^*) the average dust sample is a light colored (mean L^* of 67.3) mixture of red (mean a^* of 3.9) and yellow (mean b^* of 11.6) (figure 4). Overall, winter dust is significantly lighter (L^* of 68.7 vs. 66.3, $P = 0.007$) and yellower (b^* of 12.4 vs. 11.0, $P < 0.001$) than summer dust. The higher L^* and b^* values of summer dust are also significant when considered as paired seasonal samples for the DUST-1 through DUST-13 collectors ($P = 0.012$ and $P = 0.008$ respectively). The lowest L^* values (darkest) are at the urban samplers DUST-10 and DUST-17. Values of a^* are highest (reddest) for DUST-10, the Uinta samplers, and DUST-14, all of which are located near areas of reddish bedrock.

In XRD patterns (supplemental figure 3), all samples contain quartz (characterized by high-intensity peaks at d-spacings of 3.34 Å and 4.26 Å), albite (peaks at d-spacings of 3.19 Å and 3.21 Å), and the clay minerals illite and kaolinite (peaks at 5.0 Å and 10 Å, and 3.56 Å and 7.2 Å, respectively). The sample from DUST-14 exhibits a broad 12.5 Å peak that expands after exposure to ethylene glycol, indicative of smectite. The winter samples from

Table 1. Locations of dust collectors and durations of collections.

				Winter dust			Summer dust		
Collector	Latitude d.ddddd	Longitude d.ddddd	Elevation m	Start date d/m/yr	End date d/m/yr	Duration days	Start date d/m/yr	End date d/m/yr	Duration days
DUST-1	40.80997	−110.07345	3692	30 September 2020	2 July 2021	275	2 July 2021	10 October 2021	100
DUST-2	40.63857	−110.46599	3410	29 September 2019	29 June 2021	639	29 June 2021	24 September 2021	87
DUST-3	40.68024	−110.88894	3396	4 October 2020	9 July 2021	278	9 July 2021	28 September 2021	81
DUST-4	40.82628	−110.49868	3795	5 October 2020	8 July 2021	276	8 July 2021	27 September 2021	81
DUST-5	40.70105	−110.10081	3592	2 October 2020	30 June 2021	271	30 June 2021	8 October 2021	100
DUST-6	40.684 20	−111.029 84	3413	4 October 2020	9 July 2021	278	9 July 2021	28 September 2021	81
DUST-7	40.870 69	−110.182 56	3589	6 October 2020	7 July 2021	274	7 July 2021	26 September 2021	81
DUST-8	40.768 39	−109.834 12	3667	29 September 2020	6 July 2021	280	6 July 2021	25 September 2021	81
DUST-9	40.591 26	−111.637 70	2671	17 September 2020	28 June 2021	284	28 June 2021	21 September 2021	85
DUST-10	40.766 68	−111.828 42	1520	25 November 2020	5 July 2021	222	5 July 2021	5 October 2021	92
DUST-11	40.375 86	−115.501 40	2881	19 September 2020	27 June 2021	281	25 June 2021	4 October 2021	101
DUST-12	38.991 99	−114.317 27	3684	21 September 2020	24 June 2021	276	24 June 2021	3 October 2021	101
DUST-13	38.401 02	−112.392 93	3456	23 September 2020	10 July 2021	290	10 July 2021	2 October 2021	84
DUST-14	38.516 52	−109.218 64	3669	24 September 2020	—	—	—	01 October 2021	372
DUST-15	41.541 40	−115.966 58	3021	—	—	—	26 June 2021	15 October 2021	111
DUST-16	42.311 71	−113.651 20	2785	—	—	—	04 July 2021	16 October 2021	104
DUST-17	40.247 19	−111.650 15	1422	—	—	—	20 July 2021	11 October 2021	83

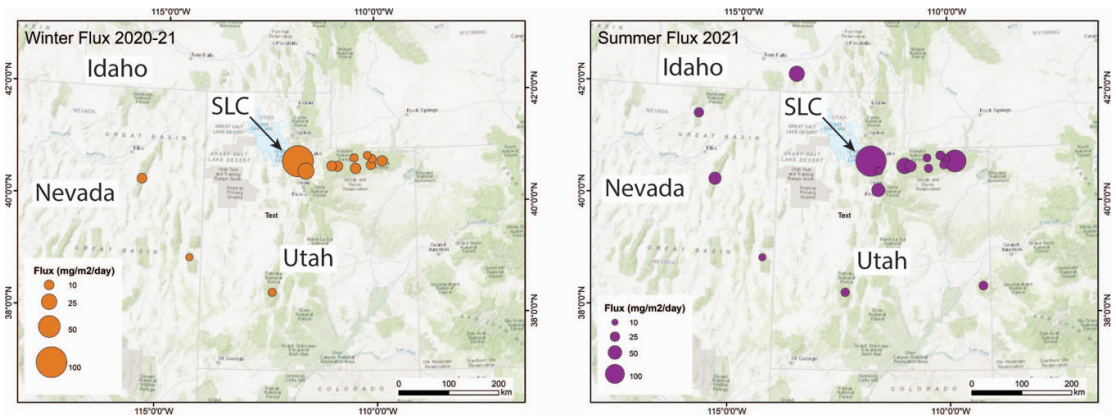

Figure 3. Maps presenting the dust flux (mg m^{-2} d^{-1}) at the 13 collectors in operation during the winter of 2020–21, and the 17 collectors operating during the summer of 2021. The states of Idaho, Nevada, and Utah are noted; SLC marks Salt Lake City.

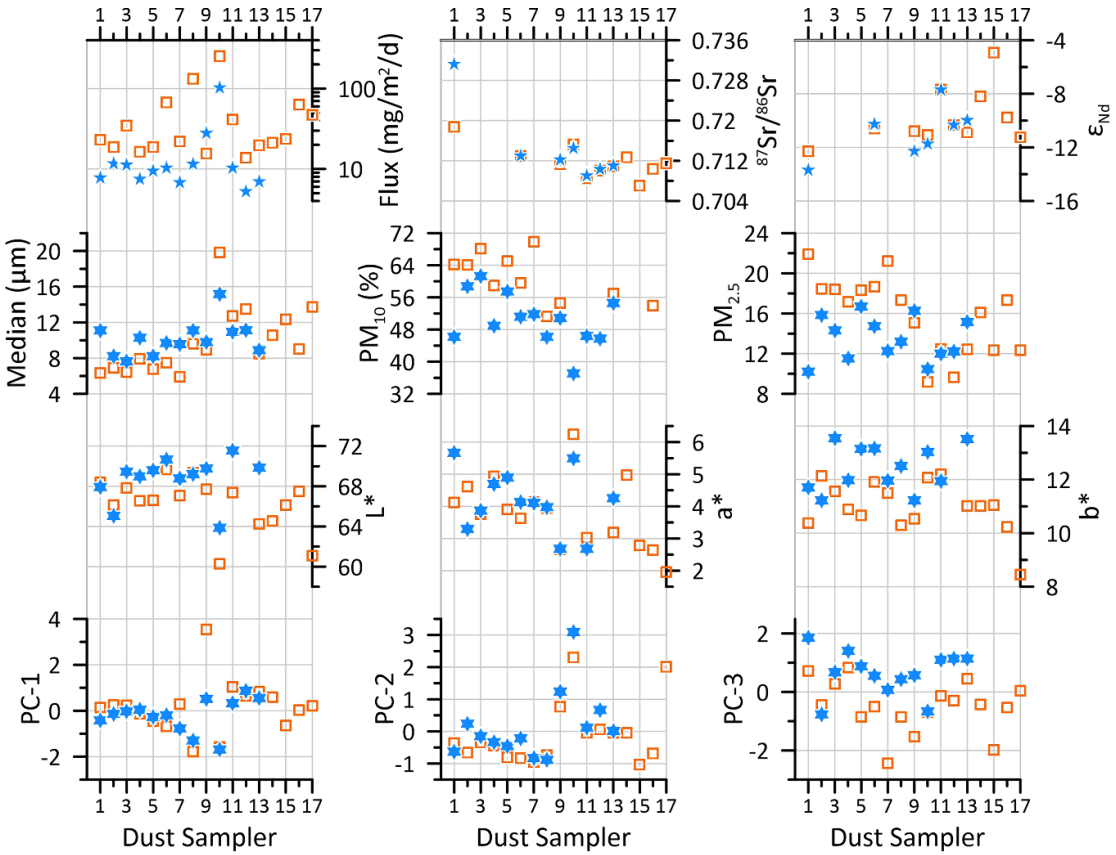

Figure 4. Plots of dust flux, $^{87}Sr/^{86}Sr$ and ε_{Nd}, median grain size, PM_{10}, $PM_{2.5}$, color in $L^*a^*b^*$ nomenclature, and the three principal components calculated for the major element chemistry of the dust samples. Blue stars are for winter 2020–21 and orange squares are summer 2021. For clarity, the annual sample from DUST-14 is plotted with the summer data. Note the logarithmic scale for dust flux.

DUST-12 and DUST-13 contain less pronounced smectite peaks that are not present in the summer samples from these locations.

After Si (not measured), the ranked abundances of major elements in the dust are Al (6.7%), Fe (3.3%), K (2.5%), Ca (1.7%), Mg (1.2%), and Ti (0.5%). The most abundant trace element is Ba (averaging 1160 ppm); Mn, Zh, Zr, Sr, Pb, and Cu are all present at average abundances >100 ppm. When normalized to Al and ratioed to average abundances in upper continental crust (Wedepohl 1995), the elements Sb, Sn, Cd, Zn, Cu, Pb, and As have enrichment factors >5×. Principle component analysis of the major elements loads Fe, Al, Ti, and Mn on PC-1, Mg and Ca on PC-2, and K on PC-3. Collectively these three components explain 80% of the variance. Values of PC-1 are lowest at DUST-10, and highest at DUST-9 (figure 4). In contrast, values of PC-2 are

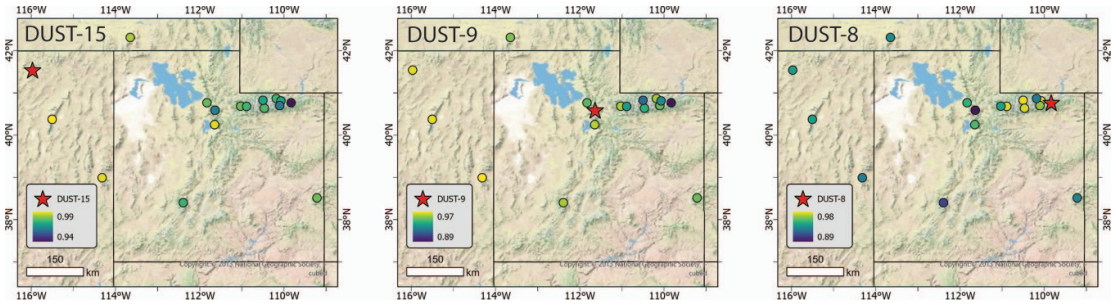

Figure 5. Maps illustrating the coefficient of determination (r^2) for all geochemical data across the collector network. DUST-15 (red star), located farthest to the northwest, exhibits the strongest correlation with collectors in Nevada (yellow) and progressively weaker correlations with collectors in southern Utah (green) and northeastern Utah (blue, black). DUST-8 (red star), at the eastern end of the Uinta Mountains, is well correlated with the other Uinta collectors, but not with sites to the west or south. DUST-9 (red star), in the Wasatch Mountains, is well correlated with collectors upwind in Nevada, but not with collectors downwind in northern Utah.

highest at DUST-10 and quite a bit lower in the Uintas and northern Nevada. The lowest PC-3 is at DUST-15. The ratio Ti/Zr is highest at DUST-9 in both seasons, and is lowest at DUST-10. In contrast, Ca/Sr is highest in both seasons at DUST-10.

Spearman rank correlations between collectors for all measured elements generally exhibit higher r^2 values for more proximal samplers, and lower values for samplers farther apart (figure 5). The most northwesterly collector, DUST-15, demonstrates the strongest correlation with other Nevada samplers, and the weakest correlation with the eastern end of the Uintas. In contrast, DUST-8 at the eastern end of the Uintas is well correlated with the other northeastern Utah samplers, but less well correlated with Nevada and southern Utah. Notably, the DUST-9 sampler in the Wasatch Mountains exhibits a strong correspondence with samplers upwind in Nevada and southern Utah, but a weaker correspondence with downwind samplers in the Uintas during both winter and summer, suggesting that the Wasatch represent a broad division between the eastern and western sectors of the studied region (figure 5).

The ratio $^{87}Sr/^{86}Sr$ in the dust ranges from 0.70707 $\pm$ 0.00001 (DUST-15 in summer) to 0.73126 $\pm$ 0.00001 (DUST-1 in winter), with an average of 0.71280 $\pm$ 0.00532 (table 2). The value of ε_{Nd} averages -10.21 ± 2.04, with the lowest value (-13.69 ± 0.32) at DUST-1 in winter, and the least negative (-4.94 ± 0.22) at DUST-15 in summer (table 2). The winter and summer samples from DUST-9 and DUST-10 fail to overlap in dual isotope space, suggesting that discrete source regions contribute dust to these locations in different seasons (figure 6). In contrast, the summer and winter samples from DUST-6, DUST-11, and DUST-12 overlap, indicating source consistency between the seasons (figure 6). Furthermore, the DUST-6 samples from the Uinta Mountains match Uinta dust (Munroe *et al* 2019) reported from previous years, indicating that the mixture of source areas dominantly contributing dust to these mountains is stable over time. The most distinct sample is DUST-15, which plots far from the others, with low $^{87}Sr/^{86}Sr$ and high ε_{Nd}, suggesting little commonality with the source regions for the other collectors.

4. Discussion

4.1. Correlations between geology and dust

Backward trajectory analysis with HYSPLIT-STILT (Lin 2003, Loughner *et al* 2021) demonstrates a strong divergence in the spatial configuration of 'hot spots' over which air passed most frequently in route to the individual collectors in different seasons. Although STILT cannot unambiguously determine if dust was entrained from a given area, it does provide a constraint on which regions are more likely to have contributed to dust transport. Hot spots for the closely spaced collectors in the Uinta Mountains overlap to a large degree, however they become increasingly discrete in the more distal parts of the collector network, with essentially no overlap for the collectors in southern Utah and eastern Nevada (figure 7). This bifurcation on either side of the Wasatch Mountains reinforces the spatial patterns seen in the geochemical data, where dust in the Uintas is internally more consistent and exhibits greater contrast with dust at sites farther away to the west and south. Seasonally, the hot spots are similar between winter and summer for DUST-6, DUST-11, and DUST-12, which exhibit similar isotope fingerprints (figure 6). The summer footprint for DUST-15 also exhibits a great deal of separation from the others, supporting the unique isotope fingerprint of dust at that site.

Intersection of these hot spots with a geologic map (supplemental figure 4) reveals major differences between dominant lithologies of the hot spots (supplemental figure 5). For example, unconsolidated Quaternary sediments comprise ~50% of the overlapping hot spots for the Uinta collectors, but this value is higher at other locations, reaching a maximum of 79% for DUST-12. Conversely, clastic

Table 2. Sr and Nd isotope results.

Field name	IGSN	Dust sampler	$^{143}Nd/^{144}Nd$ fully corr	2-SE	$\varepsilon^{143}Nd$	2-SE	$^{87}Sr/^{86}Sr$ exp norm	2-SE	Sr (mg kg^{-1})	Nd (mg kg^{-1})
Dust-1 June 2021	IEMUN000C	1	0.51193	0.000016	−13.69	0.32	0.73126	0.000012	144	27.1
Dust-6 June 2021	IEMUN001N	6	0.51211	0.000012	−10.28	0.23	0.71291	0.000011	211	30.3
Dust-9 June 2021	IEMUN0021	9	0.51200	0.000009	−12.28	0.18	0.71218	0.000011	252	30.2
Dust-10 June 2021	IEMUN0022	10	0.51203	0.000016	−11.76	0.31	0.71450	0.000009	189	24.3
Dust-11 June 2021	IEMUN0023	11	0.51224	0.000009	−7.72	0.18	0.70906	0.000011	283	26.7
Dust-12 June 2021	IEMUN0024	12	0.51210	0.000009	−10.34	0.18	0.71030	0.000011	278	32.1
Dust-13 June 2021	IEMUN0025	13	0.51212	0.000010	−9.98	0.19	0.71100	0.000009	240	35.3
Dust-1 Oct 2021	IEMUN000D	1	0.51200	0.000009	−12.28	0.17	0.71877	0.000011	203	30.6
Dust-6 Oct 2021	IEMUN001O	6	0.51209	0.000011	−10.59	0.22	0.71291	0.000009	207	27.1
Dust-9 Oct 2021	IEMUN0026	9	0.51208	0.000009	−10.79	0.18	0.71130	0.000012	252	27.1
Dust-10 Oct 2021	IEMUN0027	10	0.51207	0.000009	−11.08	0.17	0.71526	0.000015	176	23.4
Dust-11 Oct 2021	IEMUN0028	11	0.51224	0.000008	−7.69	0.16	0.70853	0.000011	257	26.8
Dust-12 Oct 2021	IEMUN0029	12	0.51210	0.000018	−10.35	0.35	0.71002	0.000011	223	28.5
Dust-13 Oct 2021	IEMUN002A	13	0.51208	0.000010	−10.87	0.19	0.71088	0.000012	202	31.2
Dust-14 Oct 2021	IEMUN002B	14	0.51221	0.000009	−8.20	0.18	0.71266	0.000011	201	37.4
Dust-15 Oct 2021	IEMUN002C	15	0.51238	0.000011	−4.94	0.22	0.70707	0.000010	221	17.8
Dust-16 Oct 2021	IEMUN002D	16	0.51213	0.000009	−9.76	0.18	0.71035	0.000010	198	30.2
Dust-17 Oct 2021	IEMUN002E	17	0.51206	0.000011	−11.25	0.22	0.71152	0.000010	284	32.4

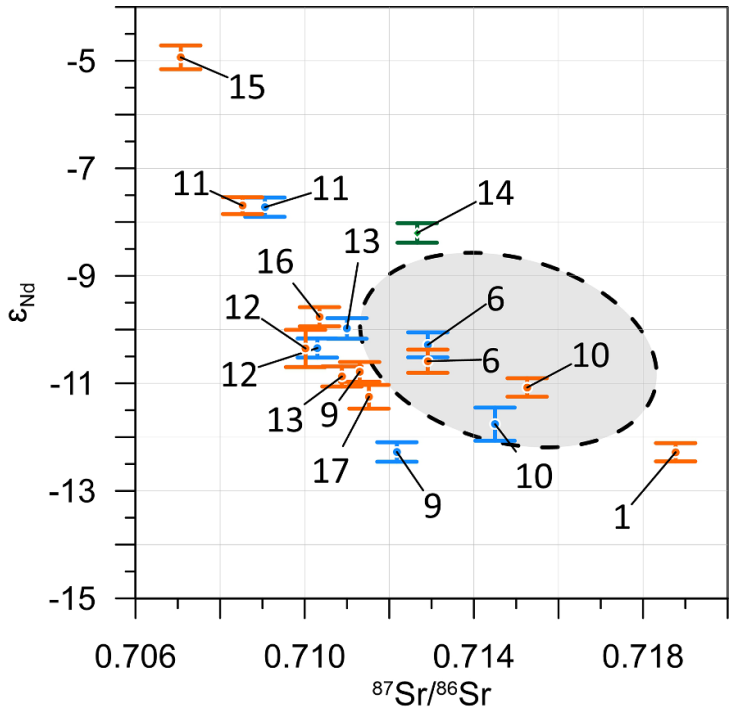

Figure 6. Biplot of $^{87}Sr/^{86}Sr$ and ε_{Nd} for representative dust samples. Blue symbols denote winter 2020–21, orange is summer 2021, and the green symbol for DUST-14 is an annual sample. The dashed gray oval highlights the range for samples reported for the Uinta Mountains in previous years (Munroe *et al* 2019, 2020).

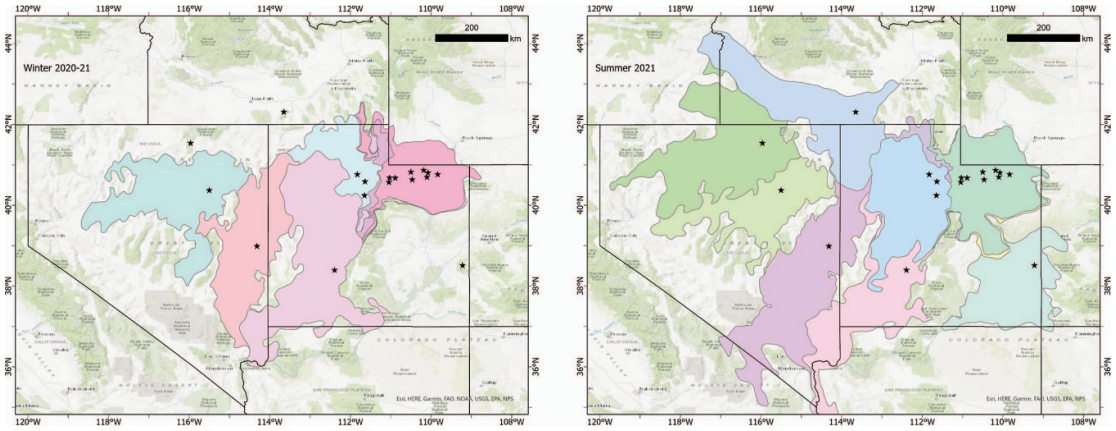

Figure 7. Maps illustrating the 'hot spots' for surrounding each collector (stars) determined through STILT backward trajectory mapping for winter 2020–21 (left) and summer 2021 (right). Hot spots generally overlap for closely spaced collectors in the Uinta Mountains of northeastern Utah, but are notably more discrete for collectors in more distal parts of the network.

sedimentary rocks comprise 32% of the Uinta hot spots, 85% of the annual hot spot for DUST-14, and just 2% at DUST-11 and DUST-12. Volcanic rock is <2% of the Uinta hot spots and for DUST-14, but >25% at DUST-15 and DUST-16.

Multiple properties analyzed for the dust samples exhibit statistically significant relationships with the extent of different lithologies. For example, the color values a^* and b^* have significant negative correlations with the area of volcanic and intrusive igneous rock, respectively. Overall dust flux has a significant positive correlation with volcanic rock, and a significant negative correlation with the area of clastic sedimentary rock and Quaternary sediment. The area of clastic sedimentary rock is also negatively correlated with Ca abundance and Ca/Sr, and positively correlated with K, La, Rb, Sc, and Rb/Sr. Collectively these observations reveal that the dust trapped by our samplers exhibits spatial variations corresponding to the geology of the surrounding lowlands.

4.2. Implications for the mountain CZ

Our investigation establishes that dust color and grain size distribution, major and trace element geochemistry, Sr and Nd isotope fingerprints, and some aspects of XRD-detectable mineralogy vary

substantially and often to a statistically significant degree between different mountain summits in the southwestern United States. Furthermore, our backward trajectory modeling demonstrates that air reaching these locations passes over areas dominated by contrasting geology. When considered in concert with the dust grain size distributions, which contain abundant fine and very fine silt, these results strongly support the hypothesis that the composition and amount of dust arriving in these mountain environments are controlled by the geology of the surrounding lowlands. Although a subordinate component of far-traveled, well-mixed dust may be present in the dust accumulating at our study sites, any homogenous background material is masked by variability stemming from regional factors.

This finding is a significant advance because previous work (e.g. Neff *et al* 2008, Skiles *et al* 2018, Carling *et al* 2020, Munroe 2022a) was not designed to evaluate the multifactor variability in dust properties between multiple mountain ranges. The few studies that did consider mountain dust over larger geographic footprints typically focused on just a single property, for instance dust concentration (Reynolds *et al* 2016), or Ca or P content (Brahney *et al* 2013, Scholz and Brahney 2022), or were restricted to just a single season (Clow *et al* 2002) rather than collecting dust year-round. Furthermore, previous efforts to evaluate the geochemical variability of broader dust source regions relied on samples collected at lower elevations (Reheis *et al* 2002, Goldstein *et al* 2008, Aarons *et al* 2017), as opposed to the mountain settings considered here. Our results, therefore, reveal for the first time the wide-ranging physical and geochemical diversity of dust reaching the ground in the mountain CZ across the southwestern United States, and emphasize the control that the geology of the surrounding landscape exerts on the composition of that dust.

This insight is germane to efforts to predict the future evolution of mountain geoecosystems due to changes in the dust cycle in southwestern North America (Shao *et al* 2011), and in locations around the world where mountain environments are influenced by dust deposition (Brahney *et al* 2019, Di Mauro *et al* 2019, Dong *et al* 2020). For instance, modeling efforts warn that arid regions in the southwestern United States are poised to become increasingly drought-prone in the future (Cayan *et al* 2010, Cook *et al* 2015, 2020, Williams *et al* 2022), a change that will likely drive shifts in the delivery of dust to the mountains (Brey *et al* 2020, Li *et al* 2021). Prior work has demonstrated that dust deposition is the primary mechanism supplying plant-available nutrients to the CZ in many mountain environments (Brahney *et al* 2013, 2014, Aciego *et al* 2017, Arvin *et al* 2017). At the locations considered in this study, the depositional rates of nutrients such as Ca and K range from 2.7 to 177 g ha^{-1} yr^{-1}, and 4.4–75 g ha^{-1} yr^{-1}, respectively, emphasizing the degree to which nutrient deposition varies in these environments under modern conditions. As the dust cycle adjusts to increasing aridity in dust emitting landscapes (Munroe 2022a), some mountain environments are likely to receive greater or lesser quantities of important nutrients than they currently do, with the potential for subsequent changes in soil fertility and geoecology. Similarly, numerous studies have illuminated the influence of dust on the timing of snowpack melting (Painter *et al* 2007, 2010, Skiles *et al* 2015), with evidence that even a single dust depositional event can accelerate final snowmelt by days to weeks (Skiles *et al* 2018, Lang *et al* 2023). Given the fundamental importance of mountain snow as a water source in the southwestern United States (Bales *et al* 2006) and other regions around the world (Huning and AghaKouchak 2020), it is critical to account for possible changes in the dust cycle when modeling future water availability (Musselman *et al* 2021, Siirila-Woodburn *et al* 2021).

5. Conclusion

Analysis of the mineral material collected by our network of dust samplers in the southwestern United States reveals striking variability in the physical and chemical properties of dust reaching the mountain CZ. This result is inconsistent with our null hypothesis that this material is globally-sourced and well-mixed (figure 1(b)). Instead, this spatial variability supports our alternate hypothesis that dust reaching these mountains is primarily sourced from surrounding lowlands with unique geologic characteristics (figure 1(c)).

This conclusion has important implications for management decisions. These landscapes are currently challenged by urbanization, livestock grazing, mining, clearing for agriculture, oil and gas development, off-road vehicle traffic, and other activities that can enhance their ability to serve as sources of dust emission (Duniway *et al* 2019). Federal entities such as the Bureau of Land Management, the US Forest Service, and the National Park Service, along with local and tribal governments, are responsible for managing these landscapes, working with consensus-driven plans that serve as guiding documents for years or decades after they are written (Forbis *et al* 2006, Başkent 2018, Brice *et al* 2020). The reality that the dust cycle directly connects decisions balancing development and protection in these landscapes, with geoecology and water availability in downwind mountains, needs to be explicitly considered in management plans moving forward.

Data availability statements

The data that support the findings of this study are openly available at the following URL/DOI: http://doi.org/10.26022/IEDA/112309 (Munroe 2022b).

Acknowledgments

Thanks to G Carling, S Lusk, D Munroe, K Perry, and A Santis for their assistance in the field, and D Fernandez for his help with the ICP-MS analysis. T Desaultel and E McMahon built the dust collectors at Middlebury College. Fieldwork for this Project took place in the ancestral homelands of the Goshute, Shoshone, and Ute tribes. This work was supported by NSF award EAR-2012082 to J Munroe, and by Middlebury College.

ORCID iDs

Jeffrey S Munroe https://orcid.org/0000-0002-9356-1899
Michael J Tappa https://orcid.org/0000-0002-9934-9100
Derek V Mallia https://orcid.org/0000-0003-1983-7305
Ann M Bauer https://orcid.org/0000-0001-7832-2112

References

Aarons S M, Arvin L J, Aciego S M, Riebe C S, Johnson K R, Blakowski M A, Koornneef J M, Hart S C, Barnes M E and Dove N 2019 Competing droughts affect dust delivery to Sierra Nevada *Aeolian Res.* **41** 100545

Aarons S M, Blakowski M A, Aciego S M, Stevenson E I, Sims K W, Scott S R and Aarons C 2017 Geochemical characterization of critical dust source regions in the American West *Geochim. Cosmochim. Acta* **215** 141–61

Aciego S M, Riebe C S, Hart S C, Blakowski M A, Carey C J, Aarons S M, Dove N C, Botthoff J K, Sims K W W and Aronson E L 2017 Dust outpaces bedrock in nutrient supply to montane forest ecosystems *Nat. Commun.* **8** 14800

Adebiyi A A, Kok J, Murray B J, Ryder C L, Stuut J-B W, Kahn R A, Knippertz P, Formenti P, Mahowald N M and García-Pando C P 2022 A review of coarse mineral dust in the Earth system *Aeolian Res.* **60** 100849

Arvin L J, Riebe C S, Aciego S M and Blakowski M A 2017 Global patterns of dust and bedrock nutrient supply to montane ecosystems *Sci. Adv.* **3** eaao1588

Ault A P, Williams C R, White A B, Neiman P J, Creamean J M, Gaston C J, Ralph F M and Prather K A 2011 Detection of Asian dust in California orographic precipitation *J. Geophys. Res. Atmos.* **116** D16

Bales R C, Molotch N P, Painter T H, Dettinger M D, Rice R and Dozier J 2006 Mountain hydrology of the western United States *Water Resour. Res.* **42** 8432

Başkent E Z 2018 A review of the development of the multiple use forest management planning concept *Int. For. Rev.* **20** 296–313

Brahney J, Ballantyne A P, Vandergoes M, Baisden T and Neff J C 2019 Increased dust deposition in New Zealand related to twentieth century Australian land use *J. Geophys. Res. Biogeosci.* **124** 1181–93

Brahney J, Ballantyne A, Kociolek P, Spaulding S, Otu M, Porwoll T and Neff J 2014 Dust mediated transfer of phosphorus to alpine lake ecosystems of the Wind River Range, Wyoming, USA *Biogeochemistry* **120** 1–20

Brahney J, Ballantyne A, Sievers C and Neff J 2013 Increasing Ca^{2+} deposition in the western US: the role of mineral aerosols *Aeolian Res.* **10** 77–87

Brey S J, Pierce J R, Barnes E A and Fischer E V 2020 Estimating the spread in future fine dust concentrations in the Southwest United States *J. Geophys. Res. Atmos.* **125** e2019JD031735

Brice E M, Miller B A, Zhang H, Goldstein K, Zimmer S N, Grosklos G J, Belmont P, Flint C G, Givens J E and Adler P B 2020 Impacts of climate change on multiple use management of Bureau of Land Management land in the Intermountain West, USA *Ecosphere* **11** e03286

Carling G T, Fernandez D P and Johnson W P 2012 Dust-mediated loading of trace and major elements to Wasatch Mountain snowpack *Sci. Total Environ.* **432** 65–77

Carling G T, Fernandez D P, Rey K A, Hale C A, Goodman M M and Nelson S T 2020 Using strontium isotopes to trace dust from a drying Great Salt Lake to adjacent urban areas and mountain snowpack *Environ. Res. Lett.* **15** 114035

Cayan D R, Das T, Pierce D W, Barnett T P, Tyree M and Gershunov A 2010 Future dryness in the southwest US and the hydrology of the early 21st century drought *Proc. Natl Acad. Sci.* **107** 21271–6

Clow D W, Ingersoll G P, Mast M A, Turk J T and Campbell D H 2002 Comparison of snowpack and winter wet-deposition chemistry in the Rocky Mountains, USA: implications for winter dry deposition *Atmos. Environ.* **36** 2337–48

Cook B I, Ault T R and Smerdon J E 2015 Unprecedented 21st century drought risk in the American Southwest and Central Plains *Sci. Adv.* **1** e1400082

Cook B I, Mankin J S, Marvel K, Williams A P, Smerdon J E and Anchukaitis K J 2020 Twenty-first century drought projections in the CMIP6 forcing scenarios *Earth's Future* **8** e2019EF001461

Creamean J M, Spackman J R, Davis S M and White A B 2014 Climatology of long-range transported Asian dust along the West Coast of the United States *J. Geophys. Res. Atmos.* **119** 12–171

Creamean J M, Suski K J, Rosenfeld D, Cazorla A, DeMott P J, Sullivan R C, White A B, Ralph F M, Minnis P and Comstock J M 2013 Dust and biological aerosols from the Sahara and Asia influence precipitation in the western US *Science* **339** 1572–8

Dahms D E 1993 Mineralogical evidence for eolian contribution to soils of late Quaternary moraines, Wind River Mountains, Wyoming, USA *Geoderma* **59** 175–96

Di Mauro B, Garzonio R, Rossini M, Filippa G, Pogliotti P, Galvagno M, Morra Di Cella U, Migliavacca M, Baccolo G and Clemenza M 2019 Saharan dust events in the European Alps: role in snowmelt and geochemical characterization *Cryosphere* **13** 1147–65

Dong Z, Brahney J, Kang S, Elser J, Wei T, Jiao X and Shao Y 2020 Aeolian dust transport, cycle and influences in high-elevation cryosphere of the Tibetan Plateau region: new evidences from alpine snow and ice *Earth-Sci. Rev.* **211** 103408

Duniway M C, Pfennigwerth A A, Fick S E, Nauman T W, Belnap J and Barger N N 2019 Wind erosion and dust from US drylands: a review of causes, consequences, and solutions in a changing world *Ecosphere* **10** e02650

Egan P A and Price M F 2017 *Mountain Ecosystem Services and Climate Change: A Global Overview of Potential Threats and Strategies for Adaptation* (UNESCO Publishing)

Fitzgerald E, Ault A P, Zauscher M D, Mayol-Bracero O L and Prather K A 2015 Comparison of the mixing state of long-range transported Asian and African mineral dust *Atmos. Environ.* **115** 19–25

Forbis T A, Provencher L, Frid L and Medlyn G 2006 Great basin land management planning using ecological modeling *Environ. Manage.* **38** 62–83

Goldstein H L, Reynolds R L, Reheis M C, Yount J C and Neff J C 2008 Compositional trends in aeolian dust along a transect across the southwestern United States *J. Geophys. Res.* **113** F2

Goodman M M, Carling G T, Fernandez D P, Rey K A, Hale C A, Bickmore B R, Nelson S T and Munroe J S 2019 Trace element chemistry of atmospheric deposition along the Wasatch Front (Utah, USA) reflects regional playa dust and local urban aerosols *Chem. Geol.* **530** 119317

Greilinger M and Kasper-Giebl A 2021 Saharan dust records and its impact in the European Alps *Oxford Research Encyclopedia of Climate Science*

Grêt-Regamey A, Brunner S H and Kienast F 2012 Mountain ecosystem services: who cares? *Mt. Res. Dev.* **32** S23–34

Grêt-Regamey A and Weibel B 2020 Global assessment of mountain ecosystem services using earth observation data *Ecosyst. Serv.* **46** 101213

Grousset F E, Ginoux P, Bory A and Biscaye P E 2003 Case study of a Chinese dust plume reaching the French Alps *Geophys. Res. Lett.* **30**

Guieu C, Loÿe-Pilot M-D, Ridame C and Thomas C 2002 Chemical characterization of the Saharan dust end-member: some biogeochemical implications for the western Mediterranean Sea *J. Geophys. Res. Atmos.* **107** ACH 5-1–11

Heindel R C, Putman A L, Murphy S F, Repert D A and Hinckley E-L S 2020 Atmospheric dust deposition varies by season and elevation in the Colorado Front Range, USA *J. Geophys. Res.* **125** e2019JF005436

Huning L S and AghaKouchak A 2020 Global snow drought hot spots and characteristics *Proc. Natl Acad. Sci.* **117** 19753–9

Kok J F, Adebiyi A A, Albani S, Balkanski Y, Checa-Garcia R, Chin M, Colarco P R, Hamilton D S, Huang Y and Ito A 2021 Improved representation of the global dust cycle using observational constraints on dust properties and abundance *Atmos. Chem. Phys.* **21** 8127–67

Lang O I, Mallia D V and Skiles S M 2023 The shrinking Great Salt Lake contributes to record high dust-on-snow deposition in the Wasatch Mountains during the 2022 snowmelt season *Environ. Res. Lett.* **18** 064045

Lawrence C R, Neff J C and Farmer G 2011 The accretion of aeolian dust in soils of the San Juan Mountains, Colorado, USA *J. Geophys. Res.* **116** F02013

Lawrence C R, Painter T H, Landry C C and Neff J C 2010 Contemporary geochemical composition and flux of aeolian dust to the San Juan Mountains, Colorado, United States *J. Geophys. Res.* **115** G03007

Lawrence C R, Reynolds R L, Ketterer M E and Neff J C 2013 Aeolian controls of soil geochemistry and weathering fluxes in high-elevation ecosystems of the Rocky Mountains, Colorado *Geochim. Cosmochim. Acta* **107** 27–46

Li Y, Mickley L J and Kaplan J O 2021 Response of dust emissions in southwestern North America to 21st century trends in climate, CO_2 fertilization, and land use: implications for air quality *Atmos. Chem. Phys.* **21** 57–68

Lin J C 2003 A near-field tool for simulating the upstream influence of atmospheric observations: the stochastic time-inverted Lagrangian transport (STILT) model *J. Geophys. Res. Atmos.* **108** ACH 2-1-ACH 2–17

Loughner C P, Fasoli B, Stein A F and Lin J C 2021 Incorporating features from the stochastic time-inverted Lagrangian transport (STILT) model into the hybrid single-particle Lagrangian integrated trajectory (HYSPLIT) model: a unified dispersion model for time-forward and time-reversed applications *J. Appl. Meteorol. Climatol.* **60** 799–810

Mahowald N, Albani S, Kok J F, Engelstaeder S, Scanza R, Ward D S and Flanner M G 2014 The size distribution of desert dust aerosols and its impact on the Earth system *Aeolian Res.* **15** 53–71

Munroe J S 2022a Relation between regional drought and mountain dust deposition revealed by a 10-year record from an alpine critical zone *Sci. Total Environ.* **844** 156999

Munroe J S 2022b Data from the DUST^2 Project, Collectors DUST-1 through DUST-17, winter 2020-21 and summer 2021, Version 1.0. Interdisciplinary Earth Data Alliance (IEDA) (https://doi.org/10.26022/IEDA/112309) (Accessed 22 September 2023)

Munroe J S, Attwood E C, O'Keefe S S and Quackenbush P J 2015 Eolian deposition in the alpine zone of the Uinta Mountains, Utah, USA *Catena* **124** 119–29

Munroe J S, McElroy R, O'Keefe S, Peters A and Wasson L 2021 Holocene records of eolian dust deposition from high-elevation lakes in the Uinta Mountains, Utah, USA *J. Quat. Sci.* **36** 66–75

Munroe J S, Norris E D, Carling G T, Beard B L, Satkoski A M and Liu L 2019 Isotope fingerprinting reveals western North American sources of modern dust in the Uinta Mountains, Utah, USA *Aeolian Res.* **38** 39–47

Munroe J S, Norris E D, Olson P M, Ryan P C, Tappa M J and Beard B L 2020 Quantifying the contribution of dust to alpine soils in the periglacial zone of the Uinta Mountains, Utah, USA *Geoderma* **378** 114631

Musselman K N, Addor N, Vano J A and Molotch N P 2021 Winter melt trends portend widespread declines in snow water resources *Nat. Clim. Change* **11** 418–24

Neff J C, Ballantyne A P, Farmer G L, Mahowald N M, Conroy J L, Landry C C, Overpeck J T, Painter T H, Lawrence C R and Reynolds R L 2008 Increasing eolian dust deposition in the western United States linked to human activity *Nat. Geosci.* **1** 189–95

Nicoll K, Hahnenberger M and Goldstein H L 2019 'Dust in the wind' from source-to-sink: analysis of the 14–15 April 2015 storm in Utah *Aeolian Res.* **46** 100532

Painter T H, Barrett A P, Landry C C, Neff J C, Cassidy M P, Lawrence C R, McBride K E and Farmer G L 2007 Impact of disturbed desert soils on duration of mountain snow cover *Geophys. Res. Lett.* **34** L12502

Painter T H, Deems J S, Belnap J, Hamlet A F, Landry C C and Udall B 2010 Response of Colorado River runoff to dust radiative forcing in snow *Proc. Natl Acad. Sci.* **107** 17125–30

Psenner R 1999 Living in a dusty world: airborne dust as a key factor for Alpine lakes *Water Air Soil Pollut.* **112** 217–27

Rea P, Ma L, Gill T E, Gardea-Torresdey J, Tamez C and Jin L 2020 Tracing gypsiferous white sands aerosols in the shallow critical zone in the northern Sacramento Mountains, New Mexico using Sr/Ca and $^{87}Sr/^{86}Sr$ ratios *Geoderma* **372** 114387

Reheis M C, Budahn J R and Lamothe P J 2002 Geochemical evidence for diversity of dust sources in the southwestern United States *Geochim. Cosmochim. Acta* **66** 1569–87

Reynolds R L, Munson S M, Fernandez D, Goldstein H L and Neff J C 2016 Concentrations of mineral aerosol from desert to plains across the central Rocky Mountains, western United States *Aeolian Res.* **23** 21–35

Routson C C, Arcusa S H, McKay N P and Overpeck J T 2019 A 4,500-year-long record of Southern Rocky Mountain dust deposition *Geophys. Res. Lett.* **46** 8281–8

Scholz J and Brahney J 2022 Evidence for multiple potential drivers of increased phosphorus in high-elevation lakes *Sci. Total Environ.* **825** 153939

Shao Y, Wyrwoll K-H, Chappell A, Huang J, Lin Z, McTainsh G H, Mikami M, Tanaka T Y, Wang X and Yoon S 2011 Dust cycle: an emerging core theme in Earth system science *Aeolian Res.* **2** 181–204

Siirila-Woodburn E R, Rhoades A M, Hatchett B J, Huning L S, Szinai J, Tague C, Nico P S, Feldman D R, Jones A D and Collins W D 2021 A low-to-no snow future and its impacts on water resources in the western United States *Nat. Rev. Earth Environ.* **2** 800–19

Skiles S M, Mallia D V, Hallar A G, Lin J C, Lambert A, Petersen R and Clark S 2018 Implications of a shrinking Great Salt Lake for dust on snow deposition in the Wasatch Mountains, UT,

as informed by a source to sink case study from the 13–14 April 2017 dust event *Environ. Res. Lett.* **13** 124031
Skiles S M, Painter T H, Belnap J, Holland L, Reynolds R L, Goldstein H L and Lin J 2015 Regional variability in dust-on-snow processes and impacts in the Upper Colorado River Basin *Hydrol. Process.* **29** 5397–413
Stuut J-B, Smalley I and O'Hara-Dhand K 2009 Aeolian dust in Europe: African sources and European deposits *Quat. Int.* **198** 234–45
Vandenberghe J 2013 Grain size of fine-grained windblown sediment: a powerful proxy for process identification *Earth-Sci. Rev.* **121** 18–30
Wedepohl K H 1995 The composition of the continental crust *Geochim. Cosmochim. Acta* **59** 1217–32
Williams A P, Cook B I and Smerdon J E 2022 Rapid intensification of the emerging southwestern North American megadrought in 2020–2021 *Nat. Clim. Change* **12** 232–4